COHERENT SYNCHROTRON RADIATION AND MICROBUNCHING IN BUNCH COMPRESSORS*

M. Borland†, ANL, Argonne, IL 60439, USA

Abstract

Coherent synchrotron radiation (CSR) is of great interest to those designing accelerators as drivers for free-electron lasers (FELs) and energy recovery linacs (ERLs). A growing body of experimental evidence indicates the potentially serious impact of CSR on beam quality as we attempt to create high-brightness, high-current electron bunches using magnetic compression techniques. It is not an overstatement to say that the success of FEL and ERL projects could well depend on how well CSR is understood in the design phase. Simulation codes typically show qualitative or rough quantitative agreement with experiments, indicating that our understanding of the physics is improving but incomplete. For example, an unexpected microbunching instability was recently discovered with the code `elegant` and is now the subject of intense theoretical work. This paper presents an overview of CSR issues, including recent simulation results on the CSR instability. Experimental results and issues are also discussed.

1 INTRODUCTION

As we seek to decrease the wavelength of the radiation from FELs, we require higher peak current and smaller emittance. Among the challenges [1] facing us are photoinjector issues such as space charge, cathode uniformity, and laser performance. Such effects determine whether we can produce a sufficiently high quality beam to begin with. Downstream of the injector, many eaffects may ruin beam quality, such as rf curvature, transverse and longitudinal wakefields, beam transport nonlinearities, and CSR.

Recently, significant progress has been made in photoinjectors (see, e.g., [2]), so the main obstacle to success for short-wavelength FELs may be beam-corrupting effects downstream of the photoinjector. In this paper, we discuss the most worrisome of these effects, namely, CSR.

CSR is of course emitted only when the beam path is bent by a dipole magnet. One way to avoid CSR is thus to eliminate dipole magnets. However, most proposals for FEL drivers [3, 4] require one or more magnetic compressors in order to achieve the required peak current. There are alternatives to standard magnetic compression, such as "emittance exchange" chicanes [5] and various velocity-based concepts [6, 7, 8], but it is unclear that these are sufficient for short x-ray FELs. Hence, the nature of CSR and its impact on beam quality seems likely to have a critical impact on the success of next-generation FELs, which will almost certainly incorporate magnetic compressors.

* Supported by the U.S. Department of Energy under contract no. W-31-109-Eng-38.

† borland@aps.anl.gov

2 NATURE OF CSR

If an electron bunch traverses a dipole field, it will emit radiation over a wide range of wavelengths. Obviously, at wavelengths long compared to the bunch length, this radiation will be coherent. The ratio of coherent to incoherent power at a wavelength λ for a Gaussian bunch of N_e electrons with rms length σ_z is [9] $C = N_e e^{-\frac{1}{2}(\frac{2\pi\sigma_z}{\lambda})^2}$. For $N_e = 6.2 \times 10^9$ (1 nC), $C \approx 16$ for $\lambda = \sigma_z$, with rapid growth as λ becomes longer. Hence, it is highly desirable to suppress radiation at wavelengths $\lambda \geq \sigma_z$, which can be done with a metallic vacuum chamber [10].

Braun *et al.* [11] give the required full chamber height g as $g \leq 1.2(\sigma_z^2\rho)^{\frac{1}{3}}$, where ρ is the bending radius. However, this specifies the chamber height that will *just begin* to attenuate CSR at wavelength $\lambda = 2\pi\sigma_z$. At this wavelength, $C \approx 4 \times 10^9$, so we believe this is insufficient. Figure 6 in [10] shows that full shielding of CSR at wavelengths above λ_s requires $g \leq 0.2(\lambda_s^2\rho)^{\frac{1}{3}}$. A conservative choice is $\lambda_s = \sigma_z$, so that C is small if shielding is not complete.

As the bunch length shrinks due to compression, the chamber gap for shielding CSR becomes impractical. In the last dipole of the first compressor in the Linac Coherent Light Source (LCLS [1]), $\rho = 2.5$ m and $\sigma_z = 190\,\mu$m, requiring $g \leq 0.9$ mm. The last dipole of the second LCLS chicane would need an even more challenging $g \leq 0.4$ mm.

Photoinjector-generated beams typically are not Gaussian, particularly when subjected to wakefields and bunch compression. These beams may have or develop nonuniformities or spikes at much smaller length scales than σ_z. As an example, suppose that we choose g to shield according to $\lambda_s = \sigma_z$ but that 10% of our 1-nC beam is in a spike of length $l_s = \sigma_z/10$. Taking $\lambda \sim l_s$, the coherent enhancement is $\sim 10^7$, with essentially no shielding. These considerations show that shielding is a difficult prospect for the kinds of beams required for x-ray FELs.

Of course, even incoherent synchrotron radiation (ISR) affects the beam. Fluctuations in energy loss (i.e., quantum excitation) degrade beam quality, since different electrons lose different amounts of energy in dipoles. CSR degrades beam quality for the same reason. However, in the case of CSR the variation in energy loss is not random but is correlated with electron position within the bunch.

The reason that the effect of CSR depends on position within the bunch is that each particle in the bunch is bathed in radiation emitted by the particles behind it. This happens even for highly relativistic particles because the electrons travel on a curved path while the photons they emit travel in straight lines. Thus, the photons can catch up to electrons in front of the emitting electron. For electrons separated by a distance s, the radiation will catch up after the beam has

traversed an angle $\phi_c(s) = (24s/\rho)^{\frac{1}{3}}$ [12].

The "overtaking length" $L_o = \rho\phi_c(\sigma_z) = (24\rho^2\sigma_z)^{\frac{1}{3}}$ gives the typical distance required for radiation to catch up. If L_o is comparable to the bending magnet length L_b, then one expects significant CSR effects on the beam. In the fourth dipole of the first and second LCLS compressor, we have, respectively, $L_o/L_b = 1.5$ and $L_o/L_b = 1.1$.

Saldin and coworkers [12] have developed a line-charge model that permits computation of the rate of CSR-induced energy modulation, commonly referred to as the "CSR wake." They give the following simple expression for the CSR wake inside the dipole, as a function of position in the bunch s and angle into the dipole ϕ:

$$\frac{dE(s,\phi)}{cdt} = T_1(s,\rho,\phi) + T_2(s,\rho,\phi), \qquad (1)$$

where

$$T_1 = K\int_{s-s_L}^{s} \frac{d\lambda}{dz}\left(\frac{1}{s-z}\right)^{\frac{1}{3}} dz, \qquad (2)$$

and

$$T_2 = K(\lambda(s-s_L) - \lambda(s-4s_L))/(s_L^{\frac{1}{3}}). \qquad (3)$$

Here, $\lambda(z)$ is the linear charge density, $s_L = (\rho\phi^3)/24$ is the slippage length, and $K = -(2e^2)/(3\rho^2)^{\frac{1}{3}}$. T_1 is the dominant term and transitions into the steady-state result in a long dipole. T_2 is an entrance transient that becomes negligible when $s_L \gg \sigma_z$.

Equations (1) through (3) are extremely convenient for simulation in a tracking code [13]. The algorithm for using these results in `elegant` [14] has been described previously [13], so we will not cover it here. The results in [12] were extended by Stupakov [15] to cover CSR propagation into the drift space following the dipole. This was first implemented by Emma [16] in a MATLAB-based code, and later added to `elegant`. `elegant` originally used less rigorous drift implementations, which generally, but not always, agree with Stupakov's method (see below).

In addition to their usefulness for simulation, significant intuitive understanding of CSR effects can be gleaned from these equations, including an understanding of the CSR microbunching instability [17]-[21].

3 CSR INSTABILITY

Inspection of equations (2) and (3) reveals that both terms have a character similar to $\frac{d\lambda}{dz}$. For $s_L \ll \sigma_z$, $T_2(s)$ is proportional to the derivative of λ at $s - 2.5 * s_L$. The appearance of $(s-z)^{\frac{-1}{3}}$ in the integrand makes T_1 similar to the derivative of λ near s. This derivative-like character can be seen in Figure 1, where we show the CSR wake for the steady-state case and Gaussian bunch. Note also that the head of the bunch gains energy while the tail loses energy. These observations lead to understanding of both energy clumping and the CSR microbunching instability.

Imagine that the beam entering a dipole has small region where the current is higher than the surroundings. Drawing on the discussion of the previous paragraph, we know

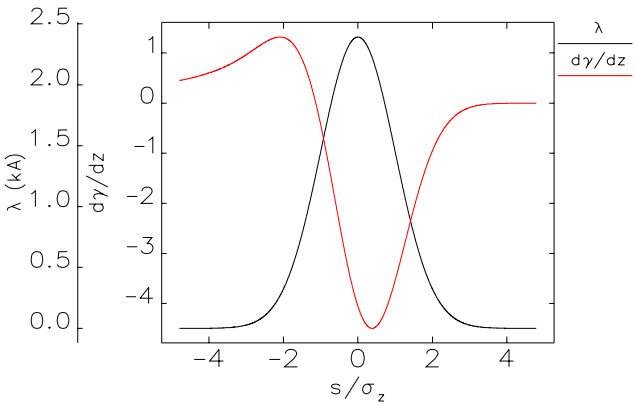

Figure 1: Example of a steady-state CSR wake for a Gaussian bunch.

that the particles ahead of this charge clump will be accelerated, while those behind it will be decelerated. Inside a dipole, a particle that gains energy falls back, while those that lose energy move forward, relative to particles at the reference energy. Hence, the combination of the CSR wake and transport in a dipole results in accentuation of the clump. This results in accentuation of the CSR wake, which results in further accentuation of the clump. Clearly, we have the potential for an instability in bunch compression systems, which was first seen in start-to-end simulation of the LCLS by Borland [17, 18].

The explanation for the formation of large-scale energy clumps [13], which are observed experimentally [22] and in simulation [13, 23], is similar to that given above. Missing from this earlier explanation is the fact that, within a single dipole, the CSR wake always results in accentuation of a density clump (in the absence of emittance and incoherent energy spread). This is seen in Figure 3 of [24], which shows instability growth in each dipole of a chicane.

3.1 Instability Gain Curves

In [18], we found that the instability in the LCLS manifested itself as a modulation in the final longitudinal phase space with a wavelength of $\sim$ 3 μm. Extensive studies showed that the instability was not a result of numerical noise in the CSR simulation. Theory [21] shows that for a perfect beam, the instability gain (the ratio of final to initial current modulation) becomes infinite as the modulation wavelength goes to zero. It also shows that, in the presence of nonzero emittance and energy spread, and for multiple bunch compressors, a peak in the gain curve occurs at nonzero wavelength, with roll-off in gain at very short wavelengths. This is plausible as a partial explanation of the appearance of a specific wavelength.

To explore this, we used `elegant` to compute CSR gain curves for a model chicane [24], with these parameters: 0.5-m-long rectangular dipoles with 2.77° bending angle; 5-m projected distance between first and second, and third and fourth dipoles; 1-m projected distance between second

and third dipoles. We assumed a 5-GeV, 6-kA beam with no initial chirp (i.e., no compression).

We varied the wavelength λ_m of a beam current modulation imposed on a flat-top current distribution of length $100\lambda_m$, with 4-σ Gaussian ends having Gaussian parameter $\sigma_e = 10\lambda_m$. These parameters were found to provide a clean central region in the pulse where the effects of the density modulation alone could be analyzed. Analysis of the modulation used Laskar's method [25], after first removing any gradual variation with a polynomial fit.

The flat-top density distribution was multiplied by the function $1 + A_m \cos(2\pi s/\lambda_m)$ to produce the modulated distribution. The modulation amplitude A_m was chosen between 2% and 0.05%, depending on the gain, as a balance between avoiding saturation (A_m too large) and controlling noise (A_m too small). A quiet-start method based on Halton sequences was used to sample this distribution. The same method was used with a Gaussian distribution to generate energy spread and transverse emittance. A bin size of $\lambda_m/20$ was used in the CSR algorithm. Use of up to 20 million simulation particles was necessary for the smallest modulation amplitudes to control noise.

Figure 2 shows gain curves for four cases along with theoretical results [21], where we assume steady-state CSR and ignore CSR in the drift spaces in order to match the assumptions of the theory. We see that in general the theory agrees well with the simulations. In most cases, the simulations predict about 20% less gain. In one case, the simulations predict 50% less gain. This discrepancy is not understood. We also see that in the practical cases with energy spread and emittance, the gain curve is peaked, although not dramatically so.

3.2 *Origin of LCLS Instability*

An interesting observation is that the PARMELA-generated longitudinal phase space used in the LCLS start-to-end simulations [17, 18] shows a small ripple, which may act as the seed for the instability. This ripple may be due to numerical problems in the PARMELA simulations [26]. On the other hand, the simulation has other idealizations such as a perfectly-shaped laser pulse that may make a larger error in the other direction.

To explore the importance of such ripple, we processed the PARMELA-generated distribution for the LCLS photoinjector to remove the ripple while preserving other properties of the beam. This involved heavy smoothing of the original longitudinal density to produce a distribution function that was then sampled using a quiet-start technique. The momentum coordinates were also replaced, either with a Gaussian random number or a quiet-start sequence. In both cases, the variation in incoherent momentum spread along the bunch was retained, in a heavily-smoothed fashion that removed ripple effects. We further processed the PARMELA-generated distribution to replace the transverse phase space data with an idealized distribution having the same slice emittance and beta functions as the original distribution, but none of the complex correlations with longitudinal coordinates.

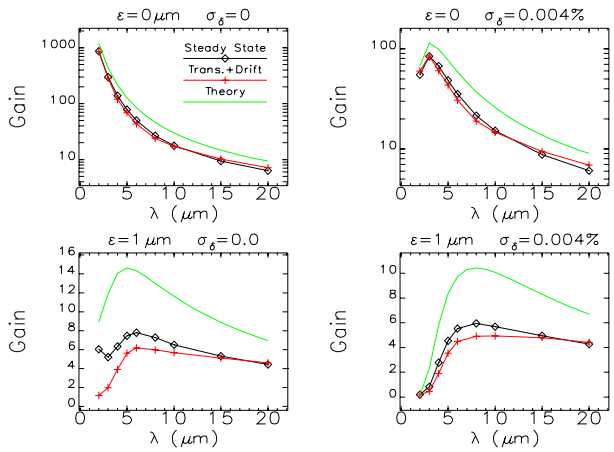

Figure 2: Comparison of simulation and theory for model chicane with various values of normalized emittance and incoherent fractional momentum spread, with 6-kA beam and no compression.

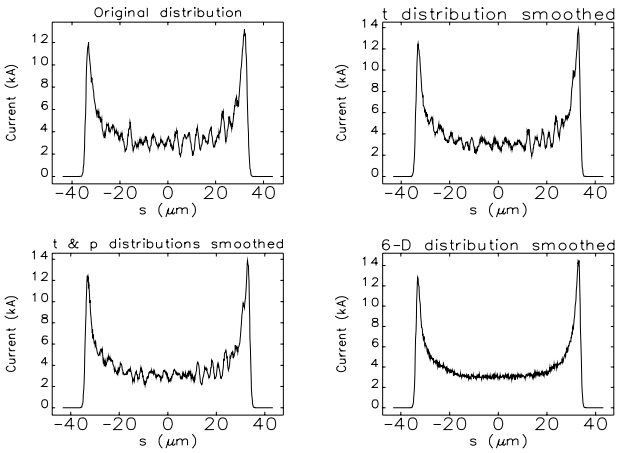

Figure 3: Comparison of LCLS final longitudinal current profiles for various degrees of smoothing of the PARMELA-generated distribution.

The longitudinal density after tracking through the LCLS for the original and three smoothed distributions are shown in Figure 3. (All LCLS tracking results include wakefields, transport nonlinearities, incoherent SR, and CSR.) If only the time distribution is smoothed, the instability is significantly reduced. If the momentum distribution is also smoothed, a nearly imperceptible change results. If the distribution is smoothed in all six dimensions, however, there is no evidence of the instability. The instability is clearly seeded by the photoinjector simulations, but not only by the longitudinal phase space. That the instability is driven by noise seems likely, although it should be remarked that the smoothing procedure removes many detailed phase space correlations as well as noise. One clear

conclusion is that the instability is not initiated by the current spikes at the head and tail of the beam.

Emma [27] reports similar results when using Gaussian input distributions. The instability is absent if particles are generated using quiet-start techniques, but present if a random number generator is used. His conclusion, which our study supports, is that the instability may not manifest itself if the photoinjector generates a very quiet distribution.

We performed additional studies to explore how ripple in the photoinjector beam due, say, to ripple in the laser temporal profile, might drive the instability. We used the 6-d smoothed distributions and added longitudinal density ripple of various wavelengths with an amplitude of 0.5%. The results of these simulations are shown in Figure 4. We see that the gain curve for the entire LCLS shows a peak at about 3 μm, which agrees with the wavelength found in the original simulations. The gain falls off rapidly below this, due no doubt to emittance and energy spread effects [21].

This gain curve allows specifying the permissible modulation of the photoinjector drive laser as a function of modulation wavelength. One must scale the wavelength to remove the compression factor. Frequency analyses of the final density distributions gives an effective compression factor for the modulation wavelength of about 0.036, compared to an expected value of 0.026 from the ratio of final to initial rms bunch length. Presumably this difference is due to nonlinearities.

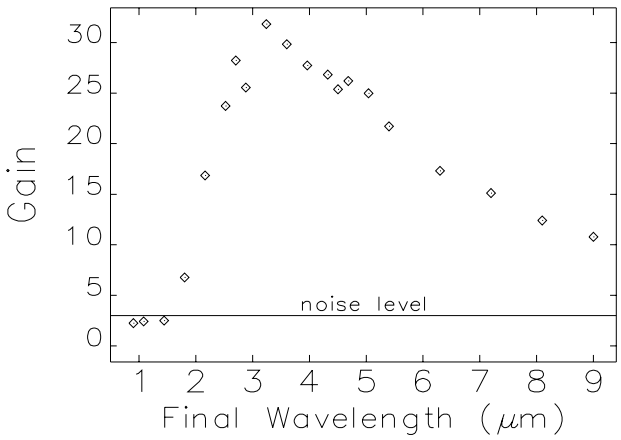

Figure 4: LCLS start-to-end CSR instability gain curve as a function of final modulation wavelength.

4 CSR EXPERIMENTS

A number of publications have reported comparisons of experiments and CSR codes [11, 28, 22], with agreement ranging from reasonable to poor. Disagreements with experiment may be due to the difficulty of knowing with sufficient precision the initial conditions of the beam entering the bunch compressor, since the details of the phase space distribution may dramatically change the CSR effects [29].

Previous comparisons [11, 28] reported for `elegant` have tended to show reasonable agreement with experiments. However, the comparisons for the CTF II experiments shown in [11] used the original drift models in `elegant`; when the Stupakov model is used, the agreement is not good. Figure 5 illustrates this, showing simulation and experimental data for the "unshielded" case (50-mm chamber gap) with a 15-nC beam (these data are not shown in [11]). For the CTF II parameters, Stupakov's result predicts a much slower decrease in the wake in the drift spaces following the dipole, which leads to enhanced effects.

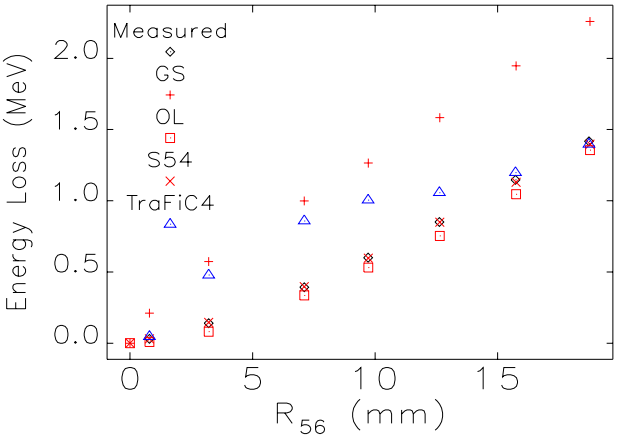

Figure 5: Comparison of CTF II experiment [11] for 50-mm chamber gap with TraFiC4 [30] and `elegant` results for various drift models: GS is Stupakov model, OL is overtaking-length model, S54 is "Saldin 54" model [13].

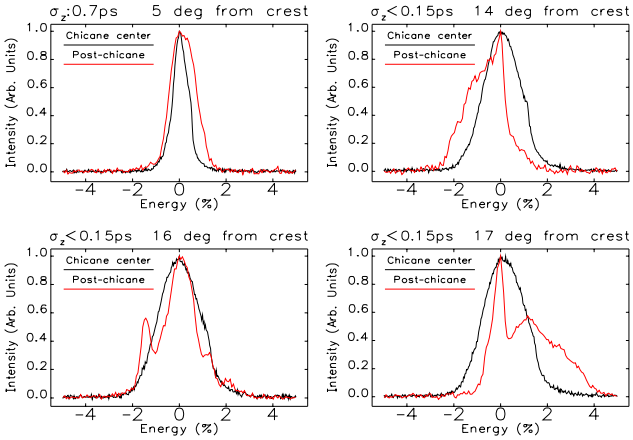

Figure 6: Typical energy spectra for APS system at chicane center and at post-chicane spectrometer for 200-pC beam.

Energy clumping, also called "phase space fragmentation" [23], has been observed at several facilities. Comparison with TraFiC^4 [30] simulations for the TTF has shown reasonable agreement with energy profiles, which provides confirmation of the basic features of the CSR wake that lead to the microbunching instability. Experiments at APS

also see energy clumping. An example of typical experimental observations is shown in Figure 6, where we see the energy spectra at the center of the chicane and on a post-chicane spectrometer for several different phases of the pre-chicane linac. Variation of the phase results in variation of the chirp, and hence variation of final bunch length.

The degree to which simulations agree with experiments at APS varies greatly among the few experiments we have performed. We attribute some of the disagreement to the difficulty we have in determining the incoming phase space from the photoinjector. Without such data, quantitative comparisons are dubious. To date, the only data for which a good determination of longitudinal phase space was possible is that shown in [28]. This is also the only experiment for which reasonable agreement is seen with simulation. Note that for the APS experiments, the different drift models agree fairly well.

Recently Loos *et al.* [31] reported microbunching structure in the beam from the Source Development Laboratory's bunch compressor. However, for the measured beam parameters, CSR instability theory predicts only modest growth. Loos *et al.* list wakefields and laser temporal structure as other possible causes of the observed microbunching. At present there is no direct experimental evidence for the microbunching instability in bunch compressors.

5 CONCLUSIONS

The effects of coherent synchrotron radiation in bunch compressors may be critical for next-generation light sources. It was recently found that CSR in bunch compressors can amplify noise or initial modulations and hence degrade beam quality significantly. Theory and simulation show general agreement on this microbunching instability. The instability might be seeded by effects like drive laser time profile nonuniformity.

Experiments show some agreement with CSR simulations in terms of prediction of phase-space fragmentation and semiquantitative features. However, experiments are fraught with difficulties that make precise comparisons difficult. Not the least of these difficulties is determining the detailed phase space of the incoming beam.

6 ACKNOWLEDGEMENTS

P. Emma (SLAC) provided LCLS input decks, a copy of his MATLAB implementation of Stupakov's model, assisted with early experiments on the APS bunch compressor, and generously shared his on-going CSR instability results. L. Groening (GSI) provided the experimental and TraFiC^4 data shown in Figure 5. Z. Huang (ANL) provided results from theory for comparison with simulations, as well as stimulating conversations on CSR. J. Lewellen (ANL) and C. Limborg (SLAC) provided PARMELA results and input decks for the LCLS photoinjector. The explanation of the CSR microbunching instability arose out of conversations with J. Rosenzweig (UCLA), Y. Schneidmiller (DESY), and G. Stupakov (SLAC). R. Soliday (ANL) specified and configured the high-performance LINUX systems that made the simulations possible.

7 REFERENCES

[1] P. Emma, Proc of EPAC 2002, Paris, France, 49 (2002).

[2] J. Yang *et al.*, Proc. of EPAC 2002, Paris, France, 1828 (2002).

[3] H. Winick *et al.*, Proc. of PAC 1993, Washington, D.C., 1445 (1994).

[4] J. Rossbach, Proc. of the PAC 1997, Vancouver, BC, 719 (1998).

[5] M. Cornacchia and P. Emma, SLAC-PUB-9225, May 2002 (2002).

[6] J.W. Lewellen and S.V. Milton, Proc. SPIE- Int. Soc. Opt. Eng., 3154 (1997) 162-171 (1998).

[7] X.J. Wang *et al.*, Proc. of the PAC 1997, Vancouver, BC, 2793 (1998).

[8] L. Serafini *et al.*, Proc. of the PAC 2001, Chicago, IL, 2242 (2001).

[9] H. Wiedemann, *Particle Accelerator Physics*, Springer-Verlag, Berlin, 1993.

[10] J.B. Murphy *et al.*, Part. Accel. 57 (1997) 9.

[11] H.H. Braun *et al.*, Proc. of PAC 2001, Chicago, IL, 164 (2001).

[12] E.L. Saldin *et al.*, NIM A 398 (1997) 392.

[13] M. Borland, Phys. Rev. ST Accel. Beams, 4, 070701, 2001.

[14] M. Borland, Advanced Photon Source LS-287, September 2000.

[15] G. Stupakov and P. Emma, SLAC LCLS-TN-01-12, 2001.

[16] P. Emma, unpublished MATLAB program.

[17] M. Borland *et al.*, Proc. of the PAC 2001, Chicago, IL, 2707 (2001).

[18] M. Borland *et al.*, NIM A 483 (2002) 268-272. IL, 2707.

[19] S. Heifets *et al.*, Phys. Rev. ST Accel. Beams 5, 064401 (2002).

[20] E.L. Saldin *et al.*, NIM A 483 (2002) 516-520.

[21] Z. Huang and K.-J. Kim, Phys. Rev. ST Accel. Beams 5, 074401 (2002).

[22] Ph. Piot *et al.*, Proc. of EPAC 2000, Vienna, Austria, 1546 (2002).

[23] T. Limberg *et al.*, NIM A 475 (2001) 353.

[24] T. Limberg *et al.*, Proc. of EPAC 2002, Paris, France, 1544 (2002).

[25] J. Laskar and A. Celletti, Physica D 56 (1992) 253.

[26] J.B. Rosenzweig, private communication.

[27] P. Emma, private communication.

[28] M. Borland and J. Lewellen, Proc. of PAC 2001, Chicago, IL, 2389 (2001).

[29] R. Li, Proc. of Linac 2000, Monterey, CA, 262 (20001).

[30] M. Dohlus *et al.*, NIM A 445 (2000) 338.

[31] H. Loos *et al.*, Proc. of EPAC 2002, Paris, France, 814 (2002).